

Variability analysis of Kuroshio intrusion through Luzon Strait using growing hierarchical self-organizing map

I-Fong Tsui & Chau-Ron Wu

Ocean Dynamics

Theoretical, Computational and
Observational Oceanography

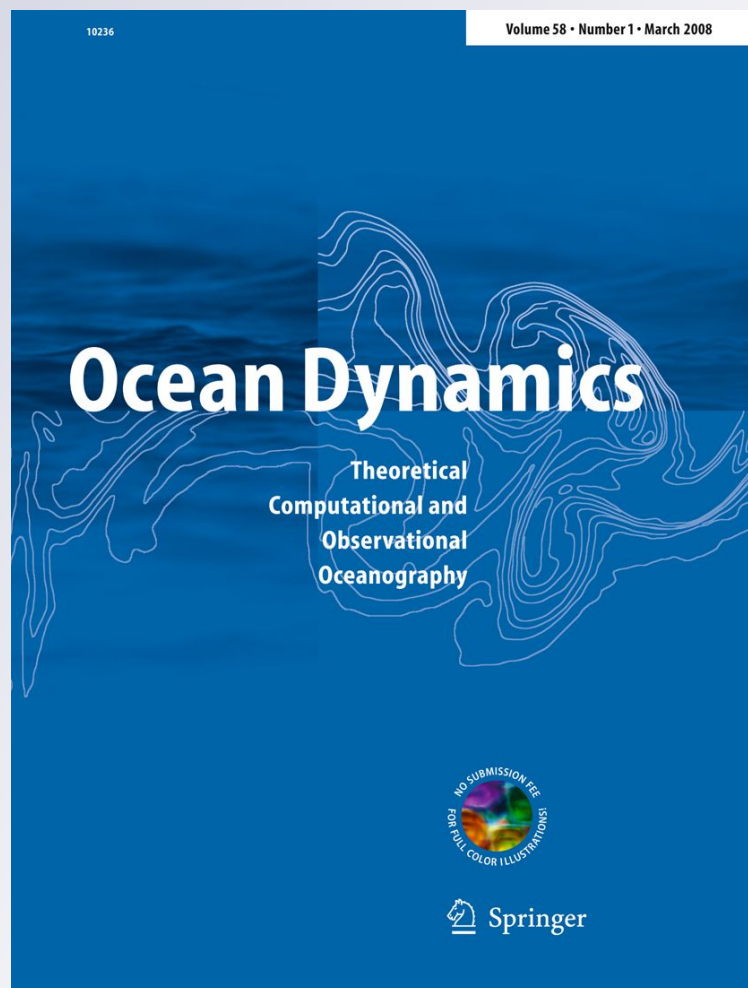
ISSN 1616-7341

Volume 62

Number 8

Ocean Dynamics (2012) 62:1187-1194

DOI 10.1007/s10236-012-0558-0



Your article is protected by copyright and all rights are held exclusively by Springer-Verlag. This e-offprint is for personal use only and shall not be self-archived in electronic repositories. If you wish to self-archive your work, please use the accepted author's version for posting to your own website or your institution's repository. You may further deposit the accepted author's version on a funder's repository at a funder's request, provided it is not made publicly available until 12 months after publication.

Variability analysis of Kuroshio intrusion through Luzon Strait using growing hierarchical self-organizing map

I-Fong Tsui · Chau-Ron Wu

Received: 6 March 2012 / Accepted: 31 May 2012 / Published online: 20 June 2012
© Springer-Verlag 2012

Abstract An advanced artificial neural network classification algorithm is applied to 18 years of gridded mean geostrophic velocity multi-satellite data to study the Kuroshio intrusion into the South China Sea through the Luzon Strait. The results suggest that the Kuroshio intrusion may occur year round. However, intrusion is not the major characteristic of the region. The intrusion mode occurs only 25.8 % of the time. Winter intrusion events are more frequent than summer events. Both stronger intrusion (which is related to wind speed) and weaker intrusion (which may be related to the upstream Kuroshio transport) may occur during winter, but stronger intrusion is dominant. In summer, the Kuroshio intrusion is almost the weaker type. The Kuroshio intrusion through the Luzon Strait usually occurs when the Pacific decadal oscillation index is positive (72.1 % of the time). This study shows that growing hierarchical self-organizing map is a useful tool for analyzing Kuroshio intrusion through the Luzon Strait.

Keywords Luzon strait · Kuroshio intrusion · Growing hierarchical self-organizing map (GHSOM) · Pacific decadal oscillation (PDO)

1 Introduction

The Kuroshio is the principal western boundary current in the North Pacific Ocean. It forms where the North Equatorial

Current bifurcates into two branches at approximately 12 °N off the east coast of the Philippines (Qu and Lukas 2003). The northward flowing branch becomes the Kuroshio, flowing along the east coast of Luzon and Taiwan (Nitani 1972). Before reaching Taiwan, the Kuroshio either intrudes into the South China Sea (SCS) or flows directly across the Luzon Strait (e.g., Wu and Chiang 2007). The Luzon Strait, which connects the Pacific Ocean and SCS, is approximately 350 km wide and at its deepest channel reaches 2500 m (Fig. 1). While water exchange between the Pacific Ocean and SCS occurs mostly through the Luzon Strait, the Kuroshio intrusion is capable of modulating circulation as well as heat and salt balances in the SCS.

The path of the Kuroshio intrusion through the Luzon Strait has been investigated using mooring arrays, drifters, and numerical model simulations. Observations reveal variation through time but are costly and available only from limited locations. Direct, long-term current measurements are often unavailable in the region. Although sea surface temperature (SST) data can be used in winter to delineate the edge of the Kuroshio by temperature difference, such data fail during summer when the surrounding SST is usually similar to that of the current. Furthermore, drifter trajectories may not well represent the Kuroshio intrusion if not deployed exactly on the intrusion path or not during the intrusion period. The intrusion pattern is also difficult to simulate by numerical models because of the complex bathymetry, monsoon variation, and the Kuroshio fluctuation in the upstream region. To improve simulations, more in situ observations and/or satellite remote sensing data are needed.

Seasonal and interannual variabilities of the Kuroshio intrusion have been reported from various observations

Responsible Editor: Jin-Song von Storch

I.-F. Tsui · C.-R. Wu (✉)
Department of Earth Sciences,
National Taiwan Normal University,
No. 88, Section 4 Ting-Chou Road,
Taipei 11677 Taiwan, Republic of China
e-mail: cwu@ntnu.edu.tw

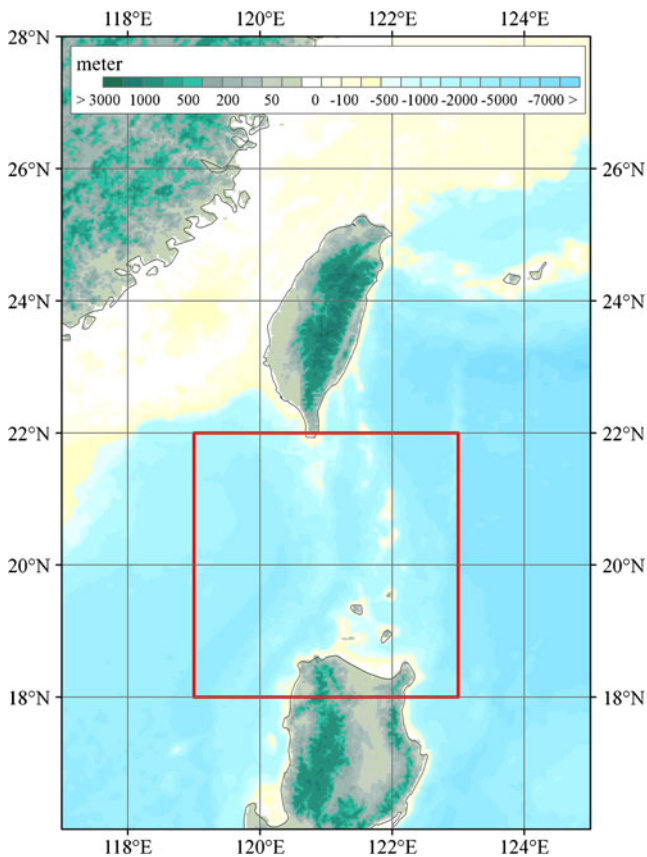


Fig. 1 Study area in the Luzon Strait

(Farris and Wimbush 1996; Wu et al. 2005; Caruso et al. 2006; Liang et al. 2008) and model simulations (Wu and Chiang 2007; Hsin et al. 2008; Hsin et al. 2012). Drifter observations during the period of 1989–2002 showed that the Kuroshio entered the SCS between October and December (Centurioni et al. 2004). According to numerical ocean model simulations, westward intrusion of the Kuroshio through the Luzon Strait is more frequent in December than in August (Wu and Chiang 2007). In summer, the Kuroshio tends to “leap” across the Luzon Strait according to model results (Sheu et al. 2010). Using SST and sea surface height (SSH) anomaly images to analyze eight winter intrusions between 1997/1998 and 2004/2005, Caruso et al. (2006) found that the Kuroshio intrusion displayed various patterns. The winter intrusion was much stronger during the winters of 1997/1998 and 1998/1999. After 4 years of weaker intrusion events, the winter intrusion became reinforced again in the winters of 2003/2004 and 2004/2005.

In addition to questions regarding the various patterns of the intrusion, it is also unclear whether the Kuroshio intrusion occurs only during the winter. A definite answer to this question has not yet to be provided because of limited observations. Liang et al. (2008) reported a likely summer

intrusion in 1998 based on moorings deployed in the Luzon Strait. However, inference from a single or even several mooring stations may not reveal the true nature of the intrusion. Yuan et al. (2006) also reported a summer Kuroshio intrusion based on visual inspection of SSH data from 1993 to 2005. However, the time period of their data was too short to confirm summer intrusion through the Luzon Strait.

Analysis of long-term, continuous remote sensing data from a large area is usually laborious. Moreover, wide-coverage products may provide synoptic images of the sea surface but poor temporal resolution compared to mooring time series. To address the problem of handling large data sets, synoptic classification is commonly used in statistical (empirical) forecasts. Recently, synoptic oceanographic classification using self-organizing map (SOM) or growing hierarchical self-organizing map (GHSOM) techniques has been adopted to identify wind and SST patterns from satellite remote data (Richardson et al. 2003; Liu et al. 2006a), coastal current patterns from Acoustic Doppler Current Profiler (ADCP) observations (Liu and Weisberg 2005), and estuary outflow patterns from high-frequency (HF) radar (Mau et al. 2007).

This study proposes the GHSOM classification procedure based on a new advanced artificial neural network classification algorithm to classify remote sensing data into meaningful flow patterns. To further understand the formation mechanism of the classified flow patterns, the patterns are correlated with wind forcing and the upstream Kuroshio transport. Interannual variability in the region was formerly attributed to the El Niño–Southern Oscillation (ENSO). However, especially in the northern Pacific Ocean, several recent studies have noticed that some oceanic phenomena are significantly influenced by the Pacific decadal oscillation (PDO) or North Pacific gyre oscillation (NPGO), rather than ENSO (e.g., Qiu and Chen 2010; Andres et al. 2009; Ceballos et al. 2009). In light of these updated findings, this study also correlates the variations derived by the GHSOM with PDO, NPGO, and ENSO to investigate the possible cause of long-term fluctuations.

2 Data and method

The present study uses SSH data instead of SST data, because oceanic dynamics are better represented by SSH than SST, which is strongly influenced by the atmosphere. Gridded altimeter-based SSH data, distributed by the Archiving, Validation and Interpretation of Satellite Oceanographic data (AVISO) service, are available from October 1992 to the present and have spatial and temporal resolutions of $1/3^\circ$ and 7 days, respectively. Gridded multi-

satellite mean geostrophic velocity (GSV) data, derived from SSH, are used to describe the flow pattern. The GSV data were validated by ship-board ADCP composite data, and mean flow patterns from the two types of data were quite similar around the Luzon Strait (Hsin et al. 2010). This study uses the U-component of the GSV from 1992 to 2009 to perform the pattern classification.

Quick Scatterometer (QuikSCAT) satellite wind data have a resolution of 0.25° in space. The data sets, which are produced by the Center for Satellite Exploitation and Research at the French Research Institute for Exploration of the Sea with rain or land flags removed, span the period from August 1999 to October 2009. This study uses weekly averages of the QuikSCAT surface wind speed data based on the date tags of the AVISO data (7 days).

Conventional empirical orthogonal function (EOF), as a linear method, may not be suitable for studying the Kuroshio intrusion. Pattern classification approaches can help identify intrusion or non-intrusion modes from remote sensing observations, which can be considered a feature extraction problem. However, it is necessary to sum up all the EOF modes to reconstruct the source data, because EOF conserves the characteristic of variation in each mode (Liu et al. 2006b). Therefore, each mode derived by EOF is only one portion of the source data. The corresponding time series contain positive and negative values which cause the flow directions in each mode to be out of phase. In this case, the flow pattern in EOF modes cannot be used to identify intrusion or non-intrusion events. As a result, EOF is not suitable as a feature extraction tool for the analysis of the intrusion problem.

A SOM is an artificial neural network based on unsupervised learning and is an effective software tool for feature extraction (Kohonen 1982, 2001). The usefulness of the method for this purpose has been demonstrated by several recent oceanic applications (Liu and Weisberg 2005; Liu et al. 2006a; Mau et al. 2007). Being worthwhile to mention, Liu et al. (2008) applied the SOM to the AVISO altimetry data (1992–2004) for the SCS and Luzon Strait. Both seasonal and interannual variations of the surface currents in the SCS were studied by Liu et al. (2008). We follow the study of Liu et al. (2008), but put more emphasis on the detailed information about the Kuroshio intrusion variability in the Luzon Strait area.

Despite its varied applications, SOM analysis has some inherent deficiencies. First, it uses a static network architecture with respect to the number and arrangement of neural nodes that have to be defined before the start of training. Second, hierarchical relationships between the input data are difficult to detect in the map display. To address both of these deficiencies within one framework, the GHSOM was recently introduced. The GHSOM consists of independent

SOMs, each of which is allowed to grow in size during the training process until a quality criterion regarding data representation is met. This growth process is continued to develop a layered architecture such that hierarchical relationships between input data are further detailed at lower layers of the neural network.

The GHSOM develops a new architecture that grows both in a horizontal and in a hierarchical way to determine the number of classification patterns and the depth of layers according to the complexity of the input data. For the interpretation of oceanographic phenomena, the number of patterns is more meaningful than the depth of layers. However, the number of classification patterns derived by the GHSOM using default parameters tends to be too high for interpretation. Moreover, using the ‘breadth’ parameter of the GHSOM to control the number of patterns is a time-consuming task. This study classifies the patterns derived with designated GHSOM parameters (breadth=0.7 and depth=0.07), which were applied in each iteration until the patterns can be examined by human eyes (pattern number ≤ 6 is recommended). In this way, the proposed method both preserves the flexibility of the GHSOM and satisfies the interpretation requirement for the outcome patterns.

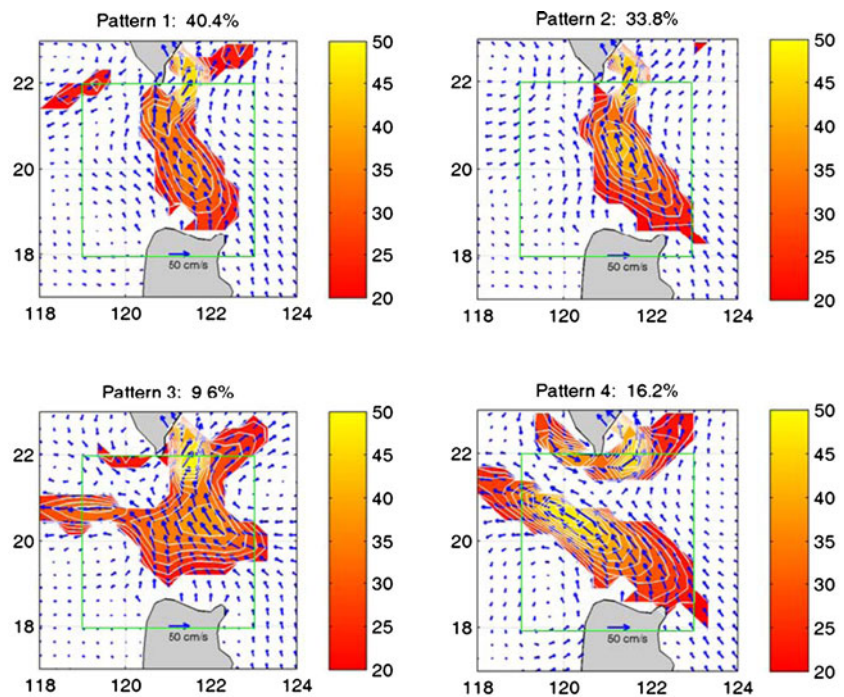
3 Results and discussion

To study the Kuroshio intrusion through the Luzon Strait, the area from approximately $18\text{--}22^\circ\text{N}$, $119\text{--}123^\circ\text{E}$ is subjected to the GHSOM analysis. Because the prevailing Kuroshio flows mainly northward in this region, the zonal component of the mean GSV is used to analyze the westward Kuroshio intrusion through the Luzon Strait. The intrusion criterion is defined as the western boundary of the 20 cm/s contour penetrating west of 120°E . Such a strict criterion has been selected to filter out any meander or loop that bypasses the Luzon Strait and does not penetrate westward into the SCS. The GHSOM analysis was applied to zonal GSV data. There are three iterations in this study. Zonal GSV data derive 63 patterns at the first iteration, 12 patterns at the second, and four patterns at the third. The final classification patterns fall into two categories, intrusion and non-intrusion. In the SOM, each piece of original data is allocated to a particular node (pattern). For each piece of data, a best-matching unit (BMU) is defined by nodes (patterns) that have the smallest weighted distance from the input data, and the BMU time series reflect the evolution of these patterns.

3.1 Classification patterns

Figure 2 shows four classification patterns. Patterns 1 and 2 are non-intrusion patterns which show the Kuroshio leaping directly northward and bypassing the SCS, except for a slight westward tendency in pattern 2. On the other hand,

Fig. 2 GHSOM-derived patterns of the Kuroshio intrusion through the Luzon Strait. The occurrence frequency of each pattern is shown at the top of each map. Green box represents the study area



patterns 3 and 4 are intrusion patterns but with different intrusion characteristics.

Pattern 3 shows a comparatively weak intrusion of the Kuroshio. The Kuroshio bifurcates in the middle of the Luzon Strait, where most of the Kuroshio water then bypasses the Luzon Strait but some Kuroshio water intrudes the SCS. This type of intrusion pattern has been reported previously. Farris and Wimbush (1996), for example, suggested that the development of the Kuroshio loop current can be divided into four stages. Caruso et al. (2006) classified three primary types of intrusions and suggested that the intrusion can evolve between the different types before returning to a mean state. Pattern 3 in this study (Fig. 2c) is similar to stage 1 of Farris and Wimbush (1996) and type 2a of Caruso et al. (2006). Pattern 4 (Fig. 2d), on the other hand, represents a strong intrusion of the Kuroshio. This pattern is similar to stage 2 of Farris and Wimbush (1996) and type 2b of Caruso et al. (2006).

Figure 2 also shows the occurrence frequency of each pattern. In general, the flow characteristic of the Kuroshio in the region is mostly the non-intrusion mode (74.2 % for pattern 1 and pattern 2). This percentage is consistent with that found by Yuan et al. (2006) using 12-year SSH data. The intrusion mode (patterns 3 and 4) occurs only about one-fourth of the time with more strong intrusion (16.2 %) than weak intrusion (9.6 %).

3.2 Seasonal variation

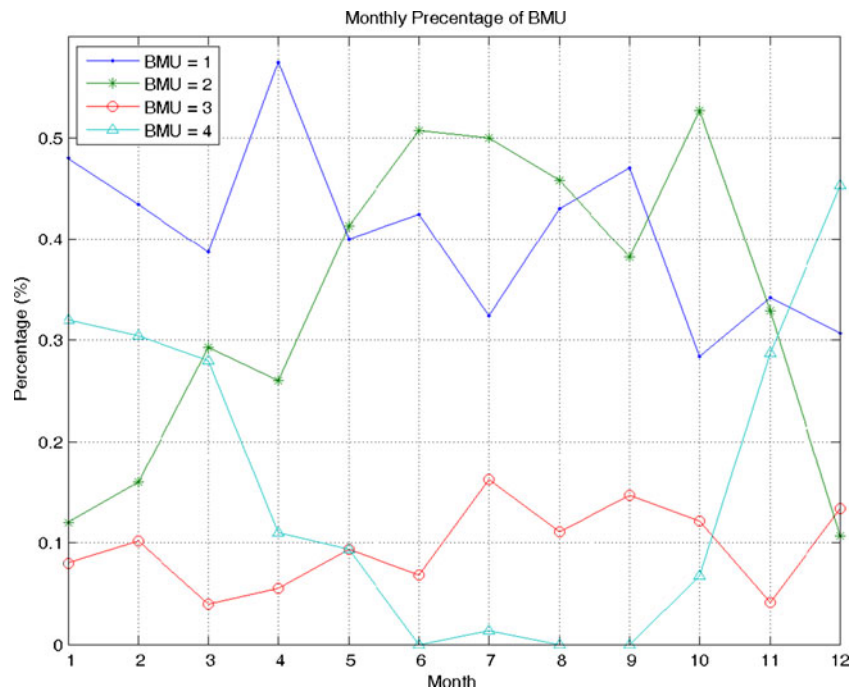
To better illustrate the monthly variability, the rate of occurrence of the four patterns was calculated. Except in

December, non-intrusion is the prevailing mode (Fig. 3). Pattern 1 occurs all year with no obvious seasonality, but pattern 2 dominates the summer-like months, May through October, with a peak in October. Pattern 3 has no significant seasonality and seldom occurs. Pattern 4 dominates the winter-like months from November to March. Pattern 2 resembles the summer circulation pattern around the Luzon Strait, whereas pattern 4 may represent winter characteristics of the region's circulation. Figure 3 also shows that the prominent Kuroshio intrusion into the SCS may take place year round, but seasonal Kuroshio intrusion occurs more often in winter than in summer. A distinctive feature of the Kuroshio intrusion is that both strong and weak intrusions occur during winter, but the strong intrusion dominates. Only a few intrusions occur during summer, and these are almost weak intrusions.

The findings about the seasonality of the Kuroshio intrusion presented in this study correspond with various observations. Philippine Sea water, for example, was found to extend west as far as 115 °E from October to January according to hydrographic data (Shaw 1991). Using advanced very high resolution radiometer SST maps, Farris and Wimbush (1996) observed that Kuroshio intrusion occurs most frequently from October to January. Centurioni et al. (2004) used drifters to demonstrate that surface water from the Philippine Sea intrudes into the SCS through the Luzon Strait between October and January when the winds are dominated by the northeast monsoon.

Comparing the results of this study with those of other observational findings reveals many consistencies regarding seasonal variations of the Kuroshio intrusion path through

Fig. 3 Monthly percentage of BMU for each pattern



the Luzon Strait. Both this study and drifter data statistical results reported in Fig. 3 of Centurioni et al. (2004) show that stronger intrusions dominate from October through March (winter-like months). Therefore, in winter, many drifter paths moved into the northern SCS through the Luzon Strait. On the other hand, in the period from April to September, besides stronger intrusion events occurred occasionally during April and May, the intrusion type is mostly weaker during summertime from June to September. The division position for bifurcation of the Kuroshio is about 20 °N, 120.8 °E. Drifter paths showed that most drifters near 20 °N were east of this division position (120.8 °E). These drifters flow northward following the main route of the Kuroshio and do not bifurcate into the northern SCS. Even some drifters approach the Luzon Strait at times; they do not flow into the northern SCS. This explains why only a few intrusions have been observed by drifters during the summer season.

To analyze the dynamic mechanism of each pattern, it is helpful to compare each pattern with individual forces. In Fig. 3, patterns 2 and 4 show significant seasonal variation and are out of phase with each other. The cause of these two patterns is subject to monsoonal winds. Located along the pathway of the East Asian monsoon system, the SCS circulation is largely influenced by the seasonal reversal of the monsoonal winds from northeasterly in winter to southwesterly in summer. Therefore, wind speed is highly correlated with the BMU of patterns 2 and 4 based on the satellite-derived wind field, with correlation coefficients of -0.56 and 0.82 , respectively, as shown in Fig. 4.

Figure 3 shows that the variation in the monthly percentage of the BMU is in a limited range for non-intrusion

pattern 1 and weaker-intrusion pattern 3. The trend of the monthly percentage of the BMU for these two patterns is correlated with the observed upstream Kuroshio transport (figure not shown). However, pattern 3 (weaker intrusion) is almost negatively correlated with the upstream Kuroshio transport.

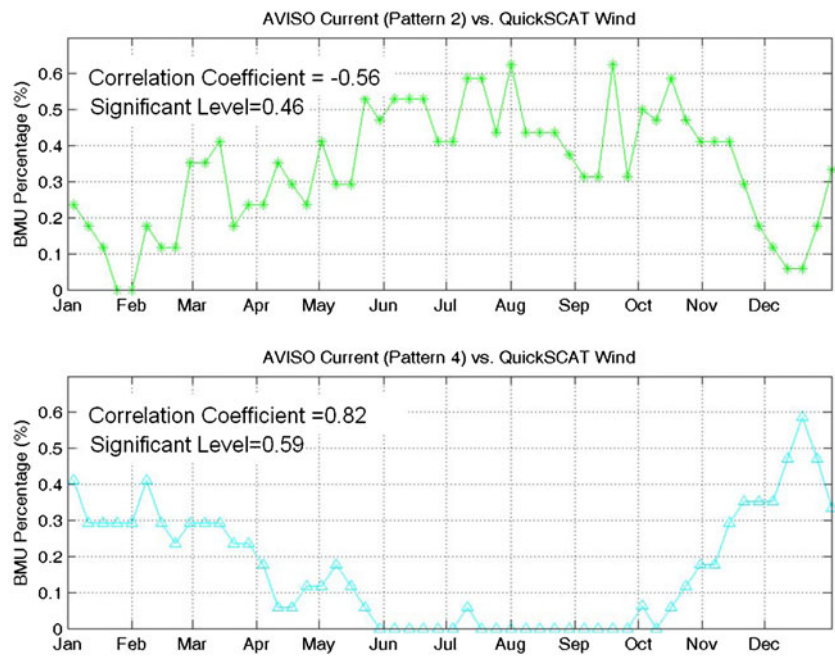
As noted in the previous two sections, the stronger intrusion of pattern 4 is related with wind speed whereas the weaker intrusion of pattern 3 is related with the upstream Kuroshio transport off the northern Luzon Island. The inertia decreases as the Kuroshio transport becomes smaller. Therefore, the Kuroshio is much more prone to intrude westward as a result of the β -effect (Sheremet 2001), which consequently can be expected to increase the occurrence frequency of pattern 3 (weaker intrusion).

3.3 Interannual variation

The BMU time series from 1993 through 2009 of the patterns derived by GHSOM is shown in Fig. 5. The BMU time series plot (Fig. 5) illustrates the interannual variation of the four patterns. As seen from the figure, the evolution of different patterns is not sequential stages as suggested by Farris and Wimbush (1996) but is similar to non-sequential stages proposed by Caruso et al. (2006) and Yuan et al. (2006).

Focusing on the Kuroshio intrusion patterns (patterns 3 and 4) in Fig. 5 (excluding the years 1992 and 2009, which do not include a full year of observation), the remaining 17 years of data can be divided into three major periods. The first period (A1) is 8 years long and extends from 1993 through 2000. It is the major intrusion period, especially of

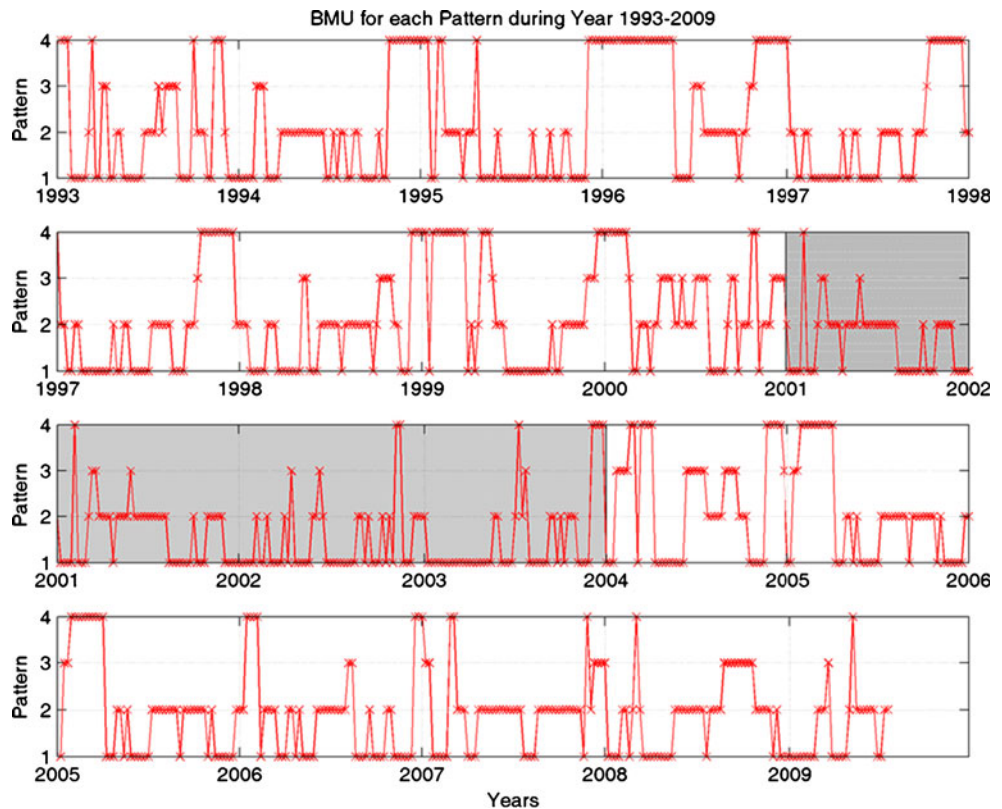
Fig. 4 Comparison between weekly-averaged AVISO BMU and QuikSCAT wind speed. Upper and lower panels show BMU percentages of pattern 2 and pattern 4, respectively



the stronger intrusion pattern (pattern 4), having a total of 33 intrusion events. Period A1 has two major features. First, winter intrusions are longer with a stronger intrusion mode. Among these, the winter of 1995/1996 has a 175-day intrusion event, which is compatible with the conclusion derived from SSH observations by Yuan et al. (2006). Second, summer intrusions are shorter, less than 28 days long. The

following period (N1) is 3 years long and extends from 2001 through 2003. Period N1 is a non-intrusion period having comparatively smaller intrusion events. During this 3-year period, there are only nine relatively short intrusion events. Excepting the 28-day intrusion event of the winter of 2003, the intrusion events are shorter than 2 weeks and have comparatively long non-intrusion events between them.

Fig. 5 Interannual variation in four patterns derived by GHSOM. Each subplot covers a 5-year period with a 1-year overlap for each subplot. The vertical axis is the pattern number



The longest non-intrusion period (315 days in 2002) occurred during this period. Subsequently, another active intrusion period (A2) that extends for 5 years from 2004 through 2008 can be recognized in Fig. 5. Although its scope is not as large as the previous 8-year intrusion period, the period is well represented by the data. Eighteen intrusion events occurred in period A2. Intrusion events occurred during each winter, except in the winter of 2008. However, these intrusion events did not exceed 28 days except for a 35-day event in the winter of 2004. Summer intrusions in this period, especially a 63-day intrusion event in August 2008, were much longer than those in winter.

To investigate the long-term trend of the Kuroshio intrusion, the correlations between the GHSOM-derived intrusion patterns (patterns 3 and 4) and long-term oscillation phenomena, such as the PDO index, NINO 3.4 index, and NPGO index, were analyzed. After comparing the results of this analysis, it was determined that the GHSOM-derived intrusion patterns have a very close relationship with the PDO index. Therefore, in this study, the BMU of intrusion patterns (3 and 4) is compared only with the PDO index, as shown in Fig. 6. Figure 6 reveals three periods: 1993–2000 (A1), 2001–2003 (N1), and 2004–2008 (A2). This result is consistent with the result derived from Fig. 5. The period N1, which is not an active intrusion period, occurs between two active intrusion periods, A1 and A2. The scale of the second active intrusion period beginning in 2004 is less than that of the previous active intrusion period. Its intrusion events distribute unequally through time. Intrusion events occurred more frequently in 2004 and 2008, respectively. The alternative three-stage pattern has a shorter period in the middle of two longer stages, which is very similar to the recent warm and cool phase of the PDO.

Table 1 shows that 60.2 and 72.1 % of intrusion events occurred when the PDO index was positive with no shift and with a 1-year time lag, respectively. Interannual variability of the Kuroshio intrusion is significant in Fig. 6. The Kuroshio intrusion occurred much more in 1996 and 1999 than the other years. On the other hand, the Kuroshio intrusion is much less common during the period between 2002 and 2003. Connected with PDO, Fig. 6 clearly shows that the

Table 1 Percentage of the positive PDO index that occurred during intrusion patterns

Lag (day)	Pattern 3 (%)	Pattern 4 (%)	Pattern 3 + 4 (%)
0	52.4	64.8	60.2
364	57.1	81.0	72.1

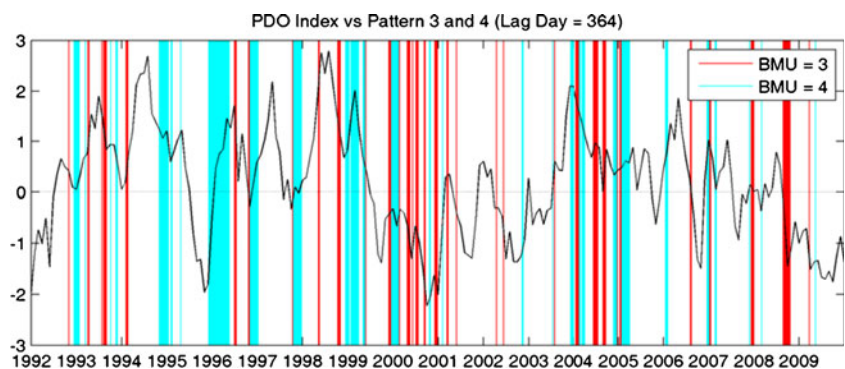
plot with a 1-year shift matches more positive PDO indices within two time periods: the non-active intrusion period from 2001 through 2003 and the active intrusion period from 2004 through 2008. Figure 6 also shows that Kuroshio intrusion occurred more frequently when the PDO index was positive, but it is necessary to explain the better relationship between the active intrusion and the PDO index when the data are shifted by 1 year. The 1-year lag may be due to ocean adjustment and feedback time after a PDO phase change. A second possibility is that the mechanism causing the PDO may need a longer amount of time to induce the Kuroshio intrusion to the SCS.

4 Concluding remarks

Analysis of 18-year AVISO GSV data reveals that the Kuroshio intrusion into the SCS through the Luzon Strait occurs throughout the year. This study represents the possibility in overcoming the limitations of the observational data length, such as by drifters and moorings. The study includes qualitative description and also quantitative analysis of the Kuroshio intrusion patterns, seasonal variations, and interannual variations in the channel between the western Pacific Ocean and the northern SCS.

This study shows that the intrusion is not a major characteristic in the study region. Based on GHSOM classification patterns, the intrusion mode (patterns 3 and 4) occurs only 25.8 % of the time. Among these, the stronger intrusion pattern (16.2 %) which is related to wind speed occurs more than the weaker intrusion pattern (9.6 %) which may be related to the upstream Kuroshio transport. These results provide a complete picture of the Kuroshio intrusion to the SCS through the Luzon Strait. Kuroshio intrusion is

Fig. 6 Overlay plot of the PDO index and intrusion patterns 3 and 4. Black solid line is the PDO index whereas the red and blue lines are the BMU of patterns 3 and 4, respectively. The plot shifts the PDO phase 1 year to match much more positive values with intrusion events



not just a single pattern. Rather, it is composed of stronger intrusion mainly in winter and weaker intrusion all year round. The intrusion does not have a specific sequence between these patterns but depends on wind speed or the upstream Kuroshio transport.

Regarding seasonal variation, winter intrusion events are more frequent than summer ones. In contrast to the weaker intrusion events which characterize summer, stronger intrusion events are usually, but not always, dominant to weaker ones in winter. Beyond a seasonal time scale, the Kuroshio intrusion demonstrates an interannual variation that is related to the PDO. The Kuroshio intrusion usually occurred when the PDO index was positive (72.1 % of the time). The results indicate the interannual variations in the Kuroshio intrusion into the SCS correlate strongly with the PDO. PDO-related studies have focused on the Kuroshio in the Kuroshio–Oyashio Extension region and northern American coastal region but rarely have been applied to the upstream Kuroshio region as in this study. Although the mechanism of the PDO is not yet fully established, this study finds that the PDO is related to the interannual variability of the Kuroshio intrusion. Effects of the PDO in the low-latitude western North Pacific should become an important topic for the future research.

In summary, it is convenient to calculate seasonal and interannual variations of oceanic or meteorological phenomena using the GHSOM. This study has proven GHSOM to be a workable tool for analysis of the Kuroshio intrusion.

In future research, the GHSOM can be applied to the other applications requiring feature extraction functionality. The Kuroshio intrusion through the Luzon Strait is the principal seawater and material exchange between the western North Pacific and the SCS. It also has a significant influence on biochemical phenomena in the SCS. The results of the study clearly demonstrate the usefulness of the GHSOM in revealing the patterns, variations, and formation mechanisms of the Kuroshio intrusion through the Luzon Strait. This study can be used as an example for studying other regions in the area.

Acknowledgments The authors would like to thank the two anonymous reviewers for their careful review of the manuscript and detailed suggestions to improve the manuscript. This research was supported by the National Science Council, Taiwan, Republic of China, under grants NSC 100-2628-M-003-001.

References

- Andres M, Park JH, Wimbush M, Zhu XH, Nakamura H, Kim K, Chang KI (2009) Manifestation of the Pacific Decadal Oscillation in the Kuroshio. *Geophys Res Lett* 36:L16602. doi:10.1029/2009GL039216
- Caruso M, Gawarkiewicz G, and Bearsley RC (2006) Interannual variability of the Kuroshio intrusion in the South China Sea. *J Oceanogr* 62:559–575
- Ceballos LI, Lorenzo ED, Hoyos CD, Schneider N, Taguchi B (2009) North Pacific gyre oscillation synchronizes climate fluctuations in the eastern and western boundary system. *J Clim* 22:5163–5174
- Centurioni LR, Niiler PP, Lee DK (2004) Observation of inflow of Philippine Sea surface water into the South China Sea through the Luzon Strait. *J Phys Oceanogr* 34:113–121
- Farris A, Wimbush M (1996) Wind-induced intrusion into the South China Sea. *J Oceanogr* 52:771–784
- Hsin YC, Wu CR, Shaw PT (2008) Spatial and temporal variations of the Kuroshio East of Taiwan, 1982–2005: a numerical study. *J Geophys Res* 113:C04002. doi:10.1029/2007JC004485
- Hsin YC, Qu T, Wu CR (2010) Intra-seasonal variation of the Kuroshio southeast of Taiwan and its possible forcing mechanism. *Ocean Dyn* 60:1293–1306. doi:10.1007/s10236-010-0294-2
- Hsin YC, Wu CR, Chao SY (2012) An updated examination of the Luzon Strait transport. *J Geophys Res* 117:C03022. doi:10.1029/2011JC007714
- Kohonen T (1982) Self-organized formation of topologically correct features maps. *Biol Cybern* 43:59–69
- Kohonen T (2001) Self-organizing maps. Springer Series in Information Sciences, Vol. 30, 3d ed., Springer-Verlag, pp 501
- Liang WD, Yang YJ, Tang TY, Chung WS (2008) Kuroshio in the Luzon Strait. *J Geophys Res* 113:C08048. doi:10.1029/2007JC004609
- Liu Y, Weisberg RH (2005) Patterns of ocean current variability on the West Florida Shelf using the self-organizing map. *J Geophys Res* 110:C06003. doi:10.1029/2004JC002786
- Liu Y, Weisberg RH, He R (2006a) Sea surface temperature patterns on the West Florida Shelf using the growing hierarchical self-organizing maps. *J Atmos Oceanic Tech* 23(2):325–338
- Liu Y, Weisberg RH, Mooers CNK (2006b) Performance evaluation of the self-organizing map for feature extraction. *J Geophys Res* 111:C05018. doi:10.1029/2005JC003117
- Liu Y, Weisberg RH, Yuan Y (2008) Patterns of upper layer circulation variability in the South China Sea from satellite altimetry using the self-organizing map. *Acta Oceanol Sin* 27(Supp):129–144
- Mau JC, Wang DP, Ullman DS, Codiga DL (2007) Characterizing long island sound outflows from HF radar using self-organizing maps. *Estuarine Coastal Shelf Sci* 74:155–165
- Nitani H (1972) Beginning of the Kuroshio. In: H. Stommel and K. Yoshida (eds) *Kuroshio—its physical aspects*, University of Tokyo Press, 129–163
- Qiu B, Chen S (2010) Eddy-mean flow interaction in the decadal modulating Kuroshio extension system. *Deep Sea Res II* 57:1098–1110
- Qu T, Lukas R (2003) The bifurcation of the north equatorial current in the Pacific. *J Phys Oceanogr* 33:5–18
- Richardson AJ, Risien C, Shillington FA (2003) Using self-organizing maps to identify patterns in satellite imagery. *Prog Oceanogr* 59:223–239
- Shaw PT (1991) The seasonal variation of the intrusion of the Philippine Sea water into the South China Sea. *J Geophys Res* 96:821–827
- Sheremet VA (2001) Hysteresis of a western boundary current leaping across a gap. *J Phys Oceanogr* 31:1247–1259
- Sheu WJ, Wu CR, Oey LY (2010) Blocking and westward passage of eddies in the Luzon Strait. *Deep Sea Res II* 57:1783–1791
- Wu CR, Chiang TL (2007) Mesoscale eddies in the northern South China Sea. *Deep Sea Res II* 54:1575–1588
- Wu CR, Tang TY, Lin SF (2005) Intra-seasonal variation in the velocity field of the northeastern South China Sea. *Cont Shelf Res* 25:2075–2083
- Yuan D, Han W, Hu D (2006) Surface Kuroshio path in the Luzon Strait area derived from satellite remote sensing data. *J Geophys Res* 111:C11007. doi:10.1029/2005JC003412